NJC

New Journal of Chemistry

An international journal of the chemical sciences

www.rsc.org/njc

Volume 32 | Number 7 | July 2008 | Pages 1081–1268

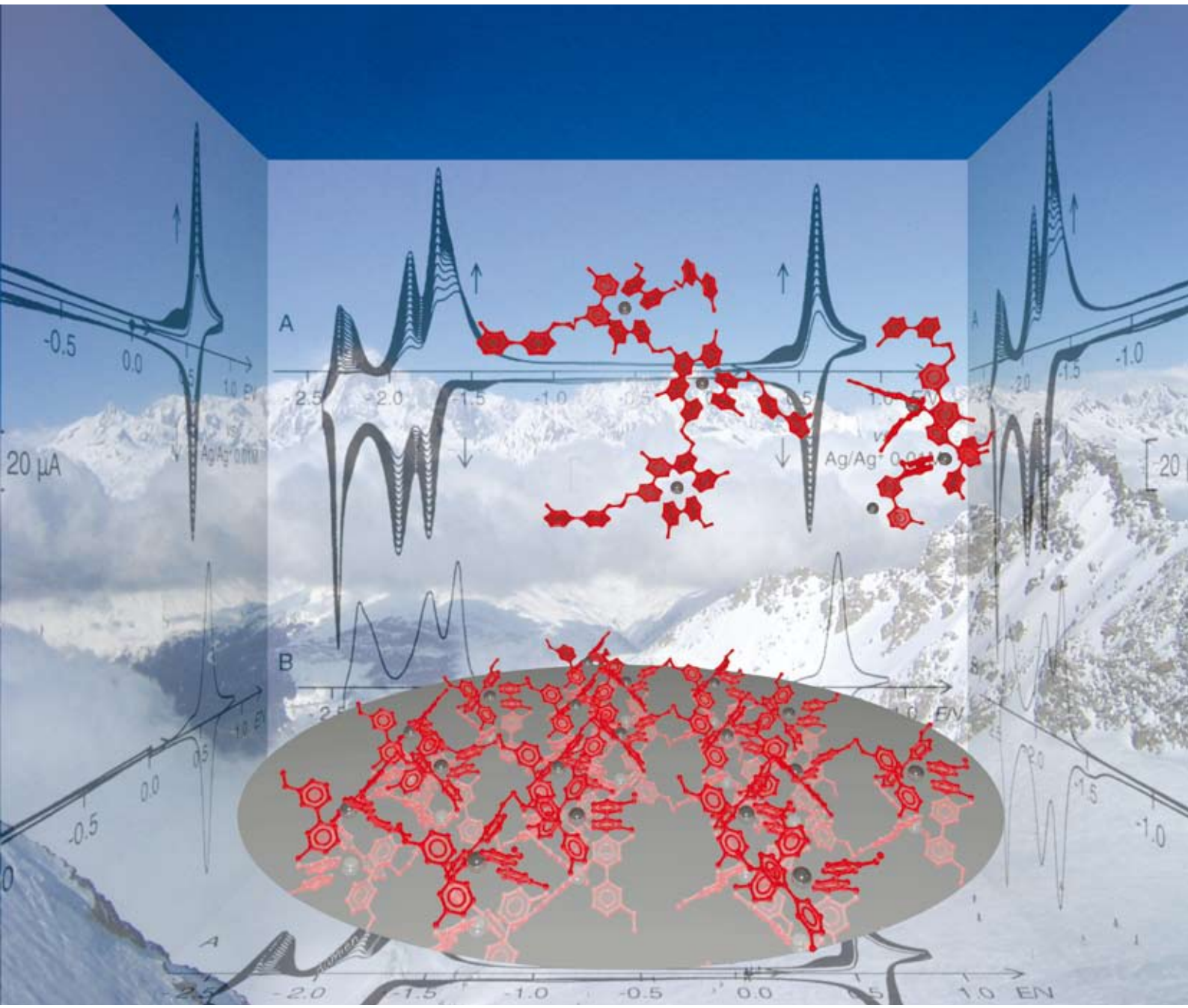

ISSN 1144-0546

RSC Publishing

CNRS CENTRE NATIONAL DE LA RECHERCHE SCIENTIFIQUE

PAPER

Marie-Noëlle Collomb *et al.*

Electrochemical behaviour of interaction between Fe^{2+} with bisbipyridyl ligands in CH_3CN

1144-0546(2008)32:7;1-0

Electrochemical behaviour of interaction between Fe^{2+} with bisbipyridyl ligands in CH_3CN. Application to an easy electrochemical procedure for tailoring films of $Fe(bpy)_3^{2+}$ like cores (bpy = 2,2′-bipyridine)

Jean Lombard, Jean-Claude Leprêtre,† Damien Jouvenot, Alain Deronzier* and Marie-Noëlle Collomb*

Received (in Montpellier, France) 27th February 2008, Accepted 26th March 2008
First published as an Advance Article on the web 18th April 2008
DOI: 10.1039/b803360a

A simple electrochemical procedure to tailor very robust thin films containing the $Fe(bpy)_3^{2+}$-like core (bpy = 2,2′-bipyridine) has been described. The procedure is based on the electroreductive precipitation of soluble macromolecules prepared *in situ* by simply mixing Fe^{2+} ions as the perchlorate salt and alkyl bridged bis-bipyridyl ligands L*n* (*n* = 2, 4, 6) in CH_3CN. NMR analyses have shown that this solution contains mainly oligomeric species but also a small amount (~5%) of low weight dinuclear $[Fe_2^{II}(Ln)_3]^{4+}$ complex. The poor solubility of the reduced forms of the oligomers causes precipitation and adsorption on the electrode surface of thin films. These films exhibit an excellent stability especially when they are cycled over the iron oxidation redox system (less than 5% loss after 80 subsequent scans). This is due to the very slow redissolution of the oxidized films.

Introduction

The coordination chemistry of alkyl bridged bipyridines and phenanthrolines (Scheme 1) has produced a large variety of dimeric and oligomeric complexes displaying interesting structures as well as new electrochemical and photochemical properties.[1–25] Numerous heterobimetallic complexes have been obtained in which the different metallic sites are connected by one of these non-conjugated ligands.[1–14] In those designs, the different active sites are maintained in close proximity without electronic connection between them. An other kind of structures are homometallic dimeric complexes of the type $[M_2(L)_2]^{n+}$ (M = Cu(I), Pd(II)) and $[M_2(L)_3]^{4+}$ (M = Fe(II), Co(II), Ru(II)), in which two and three ligands bridged the two metallic cations.[18–25]

Alkyl bridged bipyridines and phenanthrolines can also yield to the formation of oligomeric and polymeric species. However, the possibilities of tailoring self-assembled coordination polymers with such ligands have only been poorly explored,[26–30] in contrast with the extensive recent studies on related bis-terpyridine ligands.[27,29,31,32] A soluble polymer $[(Cu(L))_m]^{m+}$ has been prepared by the reaction of Cu(I) with a bis-phen ligand in which the two phenanthroline moieties are linked by an *n*-decane bridge at the 2 position (Scheme 1).[26,27] Due to the four-coordinate tetrahedral geometry of Cu(I), this polymer is one-dimensional as those formed with bis-terpyridine ligands and Fe(II), Ru(II), Co(II), or Zn(II).[27,31,32]

Using bis-bidentate ligands with metallic ions adopting an octahedral geometry, spontaneous formation of a mixture of oligomeric or polymeric species in two and/or three dimensions is expected. Such coordination polymers have not been studied in solution but have been directly formed in a solid form as thin electroactive films adsorbed on an electrode surface with Fe(II) and Co(II). One method consists on cycling the potential of a solid oxidizable electrode (iron or cobalt) in contact with ligands (L*n* (*n* = 4,5)) in solution.[29] Another method which provides ticker films consists on spin coating

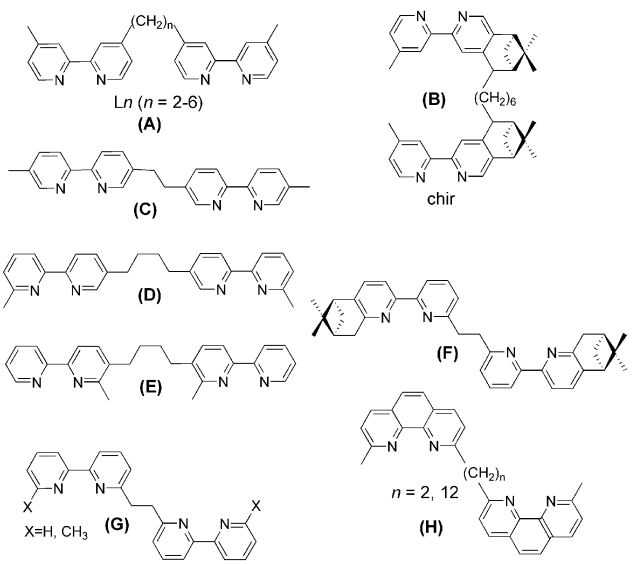

Scheme 1 Examples of some 4,4′-, 5,5′ and 6,6′-methylene-bridged bipyridine and phenanthroline ligands used in the literature, (A),[1–11,13,15,17–20,28,29] (B),[30] (C),[22,28] (D, E),[21] (F),[23] (G),[22] (H).[14,22,24,26,27]

Département de Chimie Moléculaire, UMR-5250, Institut de Chimie Moléculaire de Grenoble FR- 2607, CNRS, Université Joseph Fourier, BP-53, 38041 Grenoble, Cedex 9, France.
E-mail: alain.deronzier@ujf-grenoble.fr.
E-mail: marie-noelle.collomb@ujf-grenoble.fr
† Present address: LEPMI/ELSA/ENSEEG, Domaine Universitaire, 1130 rue de la piscine, BP75, 38042 Saint Martin d'Heres

the ligand onto an electrode, followed by its contact with a solution of the transition metal cations (Fe^{2+} or Co^{2+}).[28]

We have previously reported a different and more simple electrochemical procedure to tailor electroactive thin films of iron(II) complexes on an electrode surface.[30] The procedure is based on the *in situ* formation of soluble oligomers of a μ-oxo iron(III) binuclear complex obtained by mixing Fe^{3+} ions (as perchlorate salt) with the tetradentate bis-bipyridyl ligand (+)-chiragen (chir) (Scheme 1).[33] Depending on the experimental condition, thin films of $[Fe^{II}(chir)_{3/2}]_m^{2m+}$ or $[Fe^{II}(chir)(CH_3CN)_2]_m^{2m+}$ have been obtained by electrochemical reduction of the initial solution. The film formation is due to the poor solubility of the reduced forms of the complex. In addition the redissolution of the electrodeposited films is kinetically very slow providing their excellent electrochemical stability. Indeed, films remain adsorbed on the electrode surface even if modified electrodes are potentially cycled over the metal oxidation redox system.

In this paper we report an extension of this previous work by using a series of simpler bis-bipyridyl ligands L*n* in which the 2,2′-bipyridine moieties are connected at the 4 position by an alkyl chain of 2, 4, or 6 –(CH_2)– (Scheme 1). We have investigated the possibility of making similar films by electrochemical reduction of a solution containing a mixture of Fe^{2+} and the L*n* ligands. The electrochemical behaviour of these *in situ* made solutions of oligomers were compared with those of the isolated dimeric compounds $[Fe_2^{II}(Ln)_3]^{4+}$ (n = 2,4).[18,19]

Experimental

General

Acetonitrile (CH_3CN, Rathburn, HPLC grade) and tetra-*n*-butylammonium perchlorate (Bu_4NClO_4, Fluka) were used as received and stored under an argon atmosphere in a dry glovebox. $Fe^{II}(ClO_4)_2{\cdot}xH_2O$ (Aldrich) was used as received. The value x = 8 has been determined following a method previously described.[34] ^1H NMR spectra was recorded on a Brucker AC 250 spectrometer. UV-vis spectra were obtained using Cary 1 and Cary 100 absorption spectrophotometers on 1 mm path length quartz cells.

Synthesis

The ligands 1,2-bis[4-(4′-methyl-2,2′-bipyridinyl)]ethane (L2), 1,2-bis[4-(4′-methyl-2,2′-bipyridinyl)]butane (L4), 1,2-bis[4-(4′-methyl-2,2′-bipyridinyl)]hexane (L6) and the complexes $[Fe_2^{II}(Ln)_3](PF_6)_4$ (n = 2,4) were synthesized as previously described.[17,19]

Electrochemistry

All electrochemical measurements were run under argon in a dry glovebox at room temperature. Cyclic voltammetry were performed using an EG&G PAR model 273 potentiostat/galvanostat or an EG&G PAR model 173 potentiostat equipped with a 179 digital coulometer and a model 175 programmer, and recorded on a Sefram TGM 164 X–Y recorder. A 0.1 M solution of Bu_4NClO_4 in CH_3CN was used as supporting electrolyte. All potentials were referred to an $Ag/10^{-2}$ M $AgNO_3$ reference electrode in CH_3CN (+0.1 M Bu_4NClO_4). The potential of the regular ferrocene/ferricinium (Fc/Fc^+) redox couple used as an internal standard was $E_{1/2}$ = 87 mV under our experimental conditions. Potentials referred to $Ag/10^{-2}$ M $AgNO_3$ can be converted to SCE or NHE by adding 298 or 548 mV, respectively.[35] The working electrodes were 5 mm diameter platinum disks or 3 mm diameter vitreous carbon disks polished with 2 μm diamond paste. A Pt wire was used as counter electrode. For modified electrodes of poly/$[Fe(Ln)_{3/2}]_n^{2n+}$, the apparent surface coverage Γ (mol cm^{-2}) of electroactive species immobilized was determined from the charge under their cyclic voltammetric peaks, after the modified electrodes were transferred into a CH_3CN solution containing only the supporting electrolyte.

Results and discussion

UV-visible spectroscopy

The coordination reaction of L*n* with Fe^{2+} in CH_3CN at room temperature yields a red solution. A spectrophotometric titration of this reaction is shown in Fig. 1 for the L4 ligand. The progressive addition of $Fe^{II}(ClO_4)_2{\cdot}8H_2O$ on a solution of L*n* (0.2 mM) shows the appearance of the typical metal to ligand charge-transfer transition (MLCT) bands of Fe^{II}-tris-bipyridine complexes centered at 360 and 530 nm. Changes in the L*n* absorption was also observed upon complexation in the UV region of the spectrum with the shift of the strong ligand centered (LC) bands at 241 and 280 nm to 252 nm and 298 nm. In addition, the presence of sharply-defined isosbestic points at 234, 252, 261 and 284 nm is consistent with a single equilibrium process between two species, free L*n* and complexed L*n* (formation of a Fe(II)-tris-bipyridine complex). The titration also established the overall 1 : 1.5 stoichiometry between the Fe(II) and the ligand L*n* (Fig. 1). No change in the UV-visible

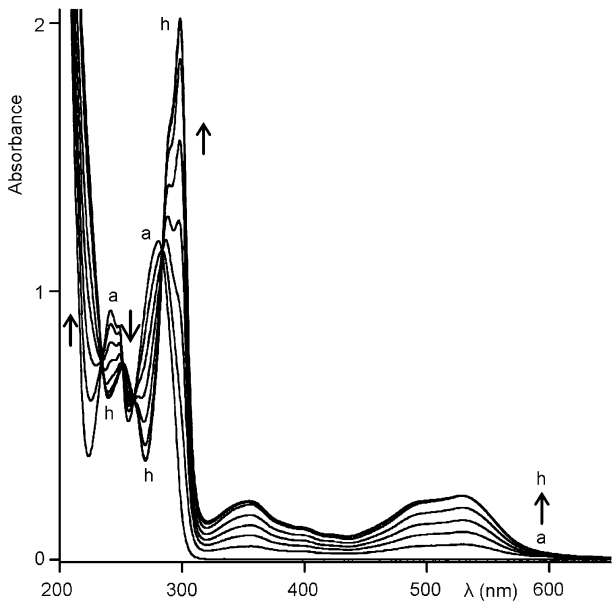

Fig. 1 Evolution of the UV-visible absorption spectrum of L4 (0.2 mM) in CH_3CN during the addition of $Fe(ClO_4)_2{\cdot}8H_2O$: (a) initial, (b) after addition of 0.1 equiv of Fe^{2+}, (c) 0.2, (d) 0.3, (e) 0.4, (f) 0.5, (g) 0.6, (h) 0.7 equiv; l = 5 mm.

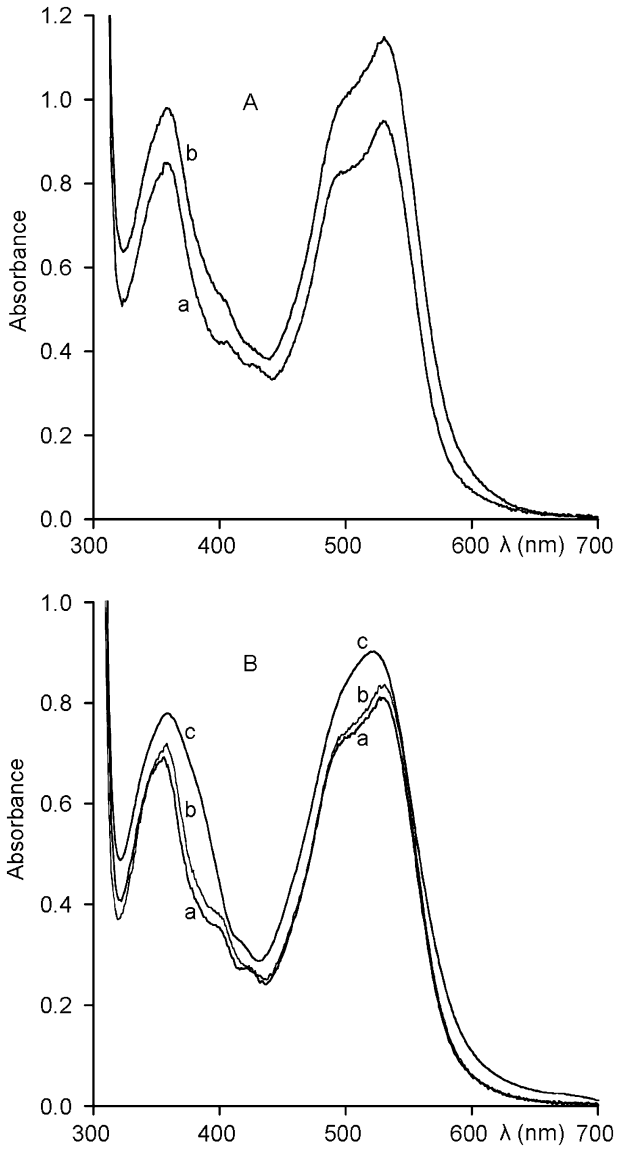

Fig. 2 Visible absorption spectra in CH_3CN of: (A) (a) $[Fe_2(L2)_3]^{4+}$ (0.51 mM), (b) Fe^{2+} (1.2 mM) + L2 (1.8 mM); (B) (a) $[Fe_2(L4)_3]^{4+}$ (0.5 mM), (b) Fe^{2+} (1 mM) + L4 (1.5 mM), (c) Fe^{2+} (1 mM) + L6 (1.5 mM); l = 1 mm.

spectra could be observed for more than 0.66 molar equivalent of Fe^{2+}.

UV-visible spectra of solutions made by simply mixing Fe^{2+} (1 mM) and L*n* (1.5 mM) in CH_3CN are shown in Fig. 2 and are compared with those of the $[Fe_2^{II}(Ln)_3]^{4+}$ complexes (n = 2, 4). The shoulders observed around 400, 420 and 495 nm are much more resolved for the dimeric species compared to the corresponding *in situ* prepared solution of Fe^{2+}/L*n*. This indicates that the species are different, as confirmed by NMR and electrochemistry (*vide infra*) with the formation of a mixture of macromolecular species (noted $[Fe^{II}(Ln)_{3/2}]_m^{2m+}$) in the case of the *in situ* made solutions. The formation of some amount of dinuclear species $[Fe_2^{II}(Ln)_3]^{4+}$ during the Fe^{2+}/L*n* complexation at room temperature cannot however be excluded. To evaluate this point NMR studies were performed.

NMR analysis

^{1}H NMR studies could provide precious information on the dimer : oligomer ratio. Comparing the spectra of $[Fe_2^{II}(Ln)_3]^{4+}$ and the freshly prepared Fe^{2+}–L*n* (1 : 1.5) solution, we were able to determine that this solution contains approximately 5% of dimer.

In the dimeric structure, the dissymmetry of the bipyridine moiety is enhanced due to the fact that the pyridine ring bearing the bridge is in close proximity to the adjacent iron complex, consequently the ring current from the facing bipyridines affects dramatically the chemical shifts (Fig. 3). The other bipyridine ring is much less affected, as it is facing outwards of the complex. Thus the "inside" protons are strongly shielded compared to the "outside" ones, with a splitting of about 1 ppm.

The spectrum of the *in situ* prepared Fe^{2+}–L*n* solution features two broad signals in the aromatic region. These broad and unresolved signals are consistent with a mixture of macromolecules. However, we can distinguish some lower intensity well-resolved peaks corresponding to $[Fe_2^{II}(Ln)_3]^{4+}$. The integration values of those peaks compared to the integration value of the broad ones allowed us to estimate the amount of dimer present in solution to *ca.* 5%. It should be pointed out however that NMR analysis is performed at higher concentration ranges than UV-visible spectroscopy or electrochemical studies.

In order to have a qualitative idea of the composition of the mixture in the concentration range of the electrochemical experiments, thin layer chromatography is a simple and fast analysis. As the possible compounds (*i.e.* the dimer and a mixture of oligomers) have the same chromophore ($Fe(bpy)_3$-like) and are intensely colored, this analysis can be regarded as semi-quantitative. TLC were performed on silica eluting with a 1 : 4 : 5, KNO_3(sat. aq.) : water : acetonitrile mixture[19] and compared to a pure sample of the dimer $[Fe_2(L2)_3]^{4+}$ previously prepared. The solution we analyzed was prepared in the same way that the ones used for the electrochemical experiments (Fe^{2+} : L2 (1 mM : 1.5 mM)). After 2 min stirring at room temperature we could already observe the formation of a small amount of dimer along with a large amount of oligomers, that, due their high charge, stay at the starting point. The evolution of the reaction mixture was followed over time, and over a period of 3 h, no significant changes were

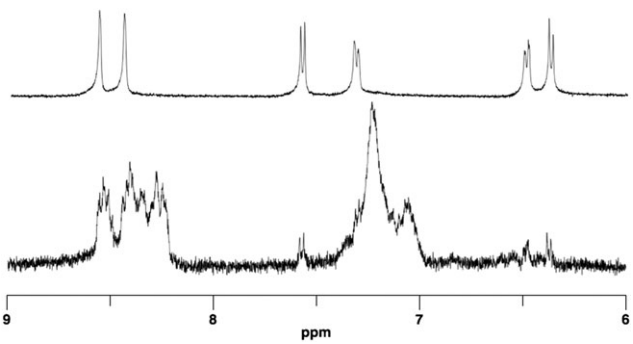

Fig. 3 NMR spectra of $[Fe_2(L2)_3]^{4+}$ (top) and of the freshly prepared Fe^{2+}/L*n* solution (bottom). Spectra are recorded in CD_3CN at 300 MHz.

observed. However, after 24 h stirring at room temperature, it appears clearly that the spot corresponding to the dimer is slightly more colored and that highly charged oligomers are still predominant.

Electrochemical studies

Redox behaviour of solutions. The redox behaviour of a Fe^{2+}–L*n* (1 : 1.5) solution was characterized by cyclic voltammetry (CV) in CH_3CN, 0.1 M Bu_4NClO_4 and compared to those of $[Fe_2^{II}(Ln)_3]^{4+}$ previously studied (*n* = 2 and 4).[19] The CV of $[Fe_2^{II}(Ln)_3]^{4+}$ displays four reversible redox processes, a metal-based Fe^{II}/Fe^{III} oxidation process in the positive potential region and three ligand-based reductions in the negative one (Fig. 4A and C). However each wave is broader compared to the mononuclear complex $[Fe(dmbpy)_3]^{2+}$, and correspond to two distinct one-electron processes. This behaviour is due to significant electrostatic interactions between the two iron centers because of the triply-bridged nature of these complexes which holds the metal centers considerably closer together than in simply linked analogs.[19] The broadening of the waves is less apparent when the number of carbons of the alkyl bridge increases. In addition, when increasing the number of methylene groups, the potential shift of each respective process relative to the mononuclear complex decreases (Table 1). By continuously cycling between 0 and −2.3 V no film deposition on the electrode surface is observed.

The CV of the solution containing a mixture of Fe^{2+} and L*n* (1 mM : 1.5 mM) shows also four reversible systems corresponding to the same redox processes as described for the dimeric complexes (Fig. 4B, D, E). However, the broadening of the Fe^{II}/Fe^{III} wave and of the first reduction one is less apparent compared to the dimeric complexes. In addition, only the first reduction wave appears to be reversible, the second reduction being complicated by adsorption which distorts the CV shape. Another notable difference compared with dimeric complexes lies in the potentials values of the various systems, the polymeric species with L2 and L4 being slightly easier to oxidize and slightly harder to reduce by approximately 60 mV.

Film deposition. As previously observed for a solution of $[Fe^{II}(chir)_{3/2}]_m^{2m+}$,[30] a rapid film growth on Pt or C electrodes occurs by continuously cycling over the three reduction systems. Fig. 5–7 show the formation of the $Pt/[Fe^{II}(Ln)_{3/2}]_m^{2m+}$ films in a potential range including the reduction systems and the oxidation system Fe^{II}/Fe^{III}. The four waves grow in and have a respective potential which corresponds closely to the potential observed in solution for the soluble species $[Fe^{II}(Ln)_{3/2}]_m^{2m+}$. If the potential range includes only the two first reduction waves the film deposition occurs but appears less efficient (Fig. 5C for L2). By cycling only on the first one, the film deposition is only poorly efficient. In contrast, if the repeated scans are limited on the wave of the reversible oxidation Fe^{II}/Fe^{III}, no deposition is observed. The efficiency of the deposition cannot be directly correlated to the length of the alkyl chain. Comparison of the CV response for the different Fe^{2+} + L*n* solutions shows that the L6 ligand exhibits the best deposition efficiency followed (in that order) by L2 and L4 (*vide infra*). For instance, after five successive

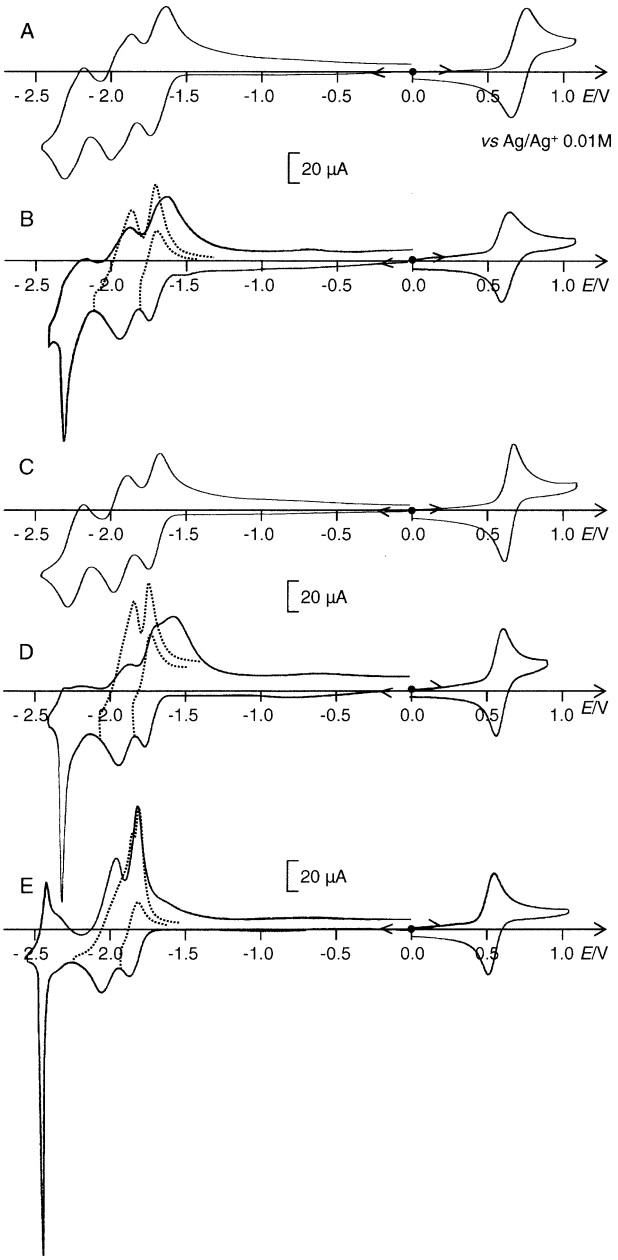

Fig. 4 Cyclic voltammograms in CH_3CN + 0.1 M Bu_4NClO_4 at a Pt electrode of (A) $[Fe_2(L2)_3]^{4+}$ (0.52 mM), (B) Fe^{2+} (1 mM) + L2 (1.5 mM), (C) $[Fe_2(L4)_3]^{4+}$ (0.52 mM), (D) Fe^{2+} (1 mM) + L4 (1.5 mM), (E) Fe^{2+} (1 mM) + L6 (1.5 mM), scan rate 100 mV s^{-1}.

cycles including the three reduction systems, the apparent surface coverage Γ of electroactive species immobilised, after transfer of the electrode into monomer-free solution (see below), is 0.45×10^{-8} mol cm^{-2} for L4, 0.82×10^{-8} for L2 and 1.2×10^{-8} for L6.

When the electrodes are removed from solution, visual examination of the surface reveals that the platinum surface is covered with a uniform dark red film. These films are similar in appearance to films formed by oxidative or reductive electropolymerization of pyrrole(bipyridine) (pyr-bpy) and vinyl(bipyridine) (v-bpy) Fe^{II} complexes.[34,36,37] The $Pt/[Fe^{II}(Ln)_{3/2}]_m^{2m+}$ modified electrode, after transfer into

Table 1 Electrochemical data for $[Fe_2(Ln)_3]^{4+}$, a mixture of $Fe^{II}(ClO_4)_2{\cdot}8H_2O$ and L*n* (1/1.5) (*in situ* formation of $[Fe^{II}(Ln)_{2/3}]_m^{2m+}$) and the corresponding modified electrodes in CH_3CN + 0.1 M Bu_4NClO_4 *vs.* Ag/Ag^+ (0.01 M $AgNO_3$ in CH_3CN + 0.1 M Bu_4NClO_4), at a scan rate of 100 mV s^{-1}

	Oxidation process	Reduction processes		
	$E_{1/2}$/V	$E_{1/2}$/V[a]		
Complexes	$Fe^{II} \leftrightarrow Fe^{III}$	1st	2nd	3rd
$[Fe(dmbpy)_3]^{2+}$[19]	0.594	−1.778	−1.966	−2.222
$[Fe_2(L2)_3]^{4+}$[19]	0.677 0.748	−1.669 −1.74	−1.913 −1.998	−2.223 −2.307
$[Fe_2(L4)_3]^{4+}$[19]	0.613 0.665	−1.699 −1.762	−1.916 −1.980	−2.217 −2.290
Fe^{2+} + 1.5 L2	0.645	−1.72	[b]	[b]
Fe^{2+} + 1.5 L4	0.58	−1.77	[b]	[b]
Fe^{2+} + 1.5 L6	0.595	−1.75	[b]	−2.35
$Pt/[Fe(L2)_{3/2}]_m^{2m+}$	0.63	−1.715	−1.90	−2.28
$Pt/[Fe(L4)_{3/2}]_m^{2m+}$	0.58	−1.755	−1.925	−2.36
$Pt/[Fe(chir)_{3/2}]_m^{2m+}$[30]	0.60	−1.72	−1.89	−2.29
$Pt/[Fe(L6)_{3/2}]_m^{2m+}$	0.595	−1.73	−1.90	−2.31

[a] Ligand-centered reduction processes. [b] This value cannot be accurately measured since the wave is strongly distorted by adsorption of the reduction product on the electrode surface (see the text).

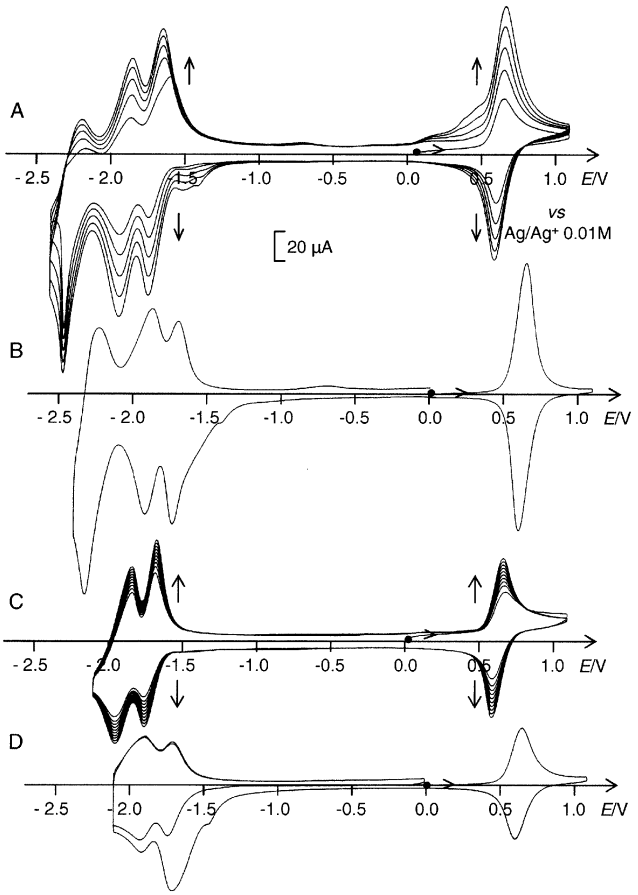

Fig. 5 (A) Elaboration of a modified electrode of a $Pt/[Fe^{II}(L2)_{3/2}]_m^{2m+}$ by five successive potential scans between 1.1 and −2.4 V from a solution of Fe^{2+} (1 mM) + L2 (1.5 mM) in CH_3CN + 0.1 M Bu_4NClO_4, (B) cyclic voltammogramms of the modified electrode prepared in (A) (Γ = 8.2 × 10^{-9} mol cm^{-2}) after transfer in CH_3CN + 0.1 M Bu_4NClO_4, (C) elaboration of a modified electrode by by ten scans between 1.1 and −2.1 V from the (A) solution, (D) cyclic voltammogramms of the modified electrode prepared in (B) (Γ = 4.9 × 10^{-9} mol cm^{-2}) after transfer in CH_3CN + 0.1 M Bu_4NClO_4; scan rate 100 mV s^{-1}.

monomer-free CH_3CN + 0.1 M Bu_4NClO_4, exhibits the same basic electrochemical behaviour as $[Fe^{II}(pyr\text{-}bpy)_3]^{2+}$ and $[Fe^{II}(v\text{-}bpy)_3]^{2+}$ films. The redox potentials of the four reversible waves observed are listed in Table 1.

Similar modified electrodes can be obtained by potentiostatic methods. The best electrodeposition efficiency is obtained when the applied potential corresponds to the second reduction process (between −1.80 and −2.05 V). From this procedure, films of 8 × 10^{-9} to 4 × 10^{-8} mol cm^{-2} were obtained for all of the ligands.

All these experiments show that the origin of the film formation is the poor solubility of the doubly reduced forms

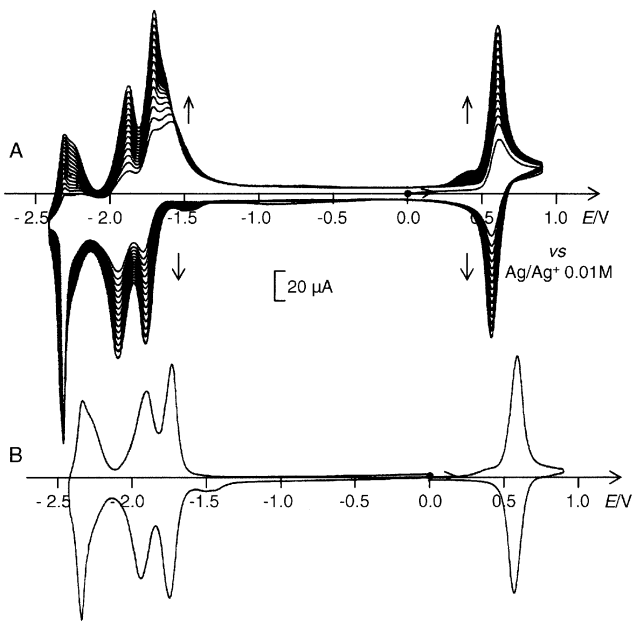

Fig. 6 (A) Elaboration of a modified electrode of a $Pt/[Fe^{II}(L4)_{3/2}]_m^{2m+}$ by 15 successive potential scans between 0.9 and −2.4 V from a solution of Fe^{2+} (1 mM) + L4 (1.5 mM) in CH_3CN + 0.1 M Bu_4NClO_4 , (B) cyclic voltammogramms of the resulting modified electrode (Γ = 6 × 10^{-9} mol cm^{-2}) after transfer in CH_3CN + 0.1 M Bu_4NClO_4; scan rate 100 mV s^{-1}.

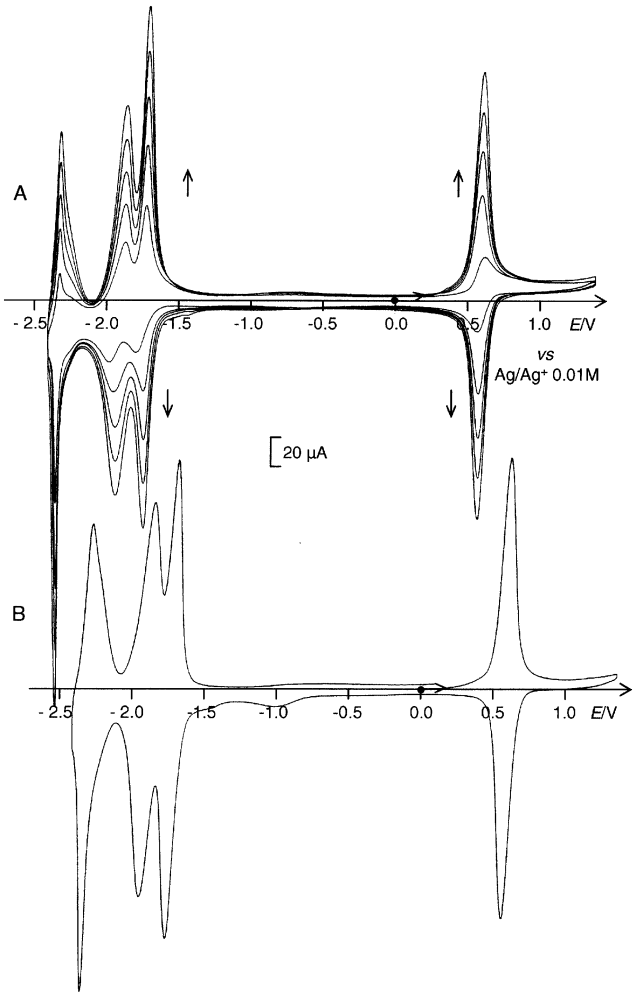

Fig. 7 (A) Elaboration of a modified electrode of a Pt/$[Fe^{II}(L6)_{3/2}]_m^{2m+}$ by five successive potential scans between 1.4 and −2.4 V from a solution of Fe^{2+} (1 mM) + L6 (1.5 mM) in CH_3CN + 0.1 M Bu_4NClO_4, (B) cyclic voltammogramms of the resulting modified electrode ($\Gamma = 9.5 \times 10^{-9}$ mol cm^{-2}) after transfer in CH_3CN + 0.1 M Bu_4NClO_4; scan rate 100 mV s^{-1}.

of the oligomeric species, $[Fe^{II}(Ln)_{3/2}]_m^0$, inducing their strong adsorption (after precipitation) on the electrode surface. In contrast, for the dimeric complexes, electrodeposition does not occur by reductive scanning which confirms unambiguously the macromolecular nature of the *in situ* formed species.

A similar behaviour, *i.e.* film formation by electroreductive precipitation, has been previously observed for hydrophobic ruthenium(II) tris-bipyridine complexes where one, two or three bpy ligand are linked to polypyrrole groups through a long (C_{13}) alkyl chain.[38,39] In such cases, the reductive electrodeposition is effective either from these soluble monomeric complexes or from their soluble corresponding polymers, synthesized by electrooxidative or photoredox polymerization.

Stability of the poly$[Fe^{II}(Ln)_{3/2}]_m^{2m+}$ films

Modified electrodes prepared by both methods exhibit toward electrochemical cycling between the Fe(II) and Fe(III) states an excellent stability, comparable to those obtained with a polypyrrole or polyvinyl backbone.[34,36,37]

About 10% loss of integrated peak current is typically observed after 20 cycles at 100 mV s^{-1} between 0 and 0.95 V while the intensity of the signal remains almost constant for 80 subsequent anodic scans (less than 5% loss).

Films are less stable towards multiple reductive scans. Typically, 50 successive scans at 100 mV s^{-1} under the first reduction wave (0 to −1.8 V) result in the loss of about 10–15% for L2 and L4 and 25% for L6 of the electroactivity of the film, as estimated from the charge measured under the ligand reduction waves. When the scanning range involves the second reduction wave (0 to −2.1 V) the loss of electroactivity can reach 50% after 50 scans in all cases.

Conclusions

We have illustrated here the perspective offered by a very useful electrochemical method to tailor thin films containing $[Fe^{II}(bpy)_{3/2}]_m^{2m+}$ like-cores from a simple mixing of Fe^{2+} and a tetradentate ligand in CH_3CN. Extension of this procedure using other metallic cations such as Co^{2+} and Mn^{2+} is currently underway.

Acknowledgements

MNC and DJ thank the Agence Nationale pour la Recherche (Grant No. ANR-05-JCJC-0171-01 (Polycomsa)) for financial support.

References

1. R. H. Schmehl, R. A. Auerbach, W. F. Wacholtz, C. M. Elliott, R. A. Freitag and J. W. Merkert, *Inorg. Chem.*, 1986, **25**, 2440.
2. F. Lafolet, J. Chauvin, M.-N. Collomb, A. Deronzier, H. Laguitton-Pasquier, J.-C. Leprêtre, J.-C. Vial and B. Brasme, *Phys. Chem. Chem. Phys.*, 2003, **5**, 2520.
3. J. Lombard, S. Romain, S. Dumas, J. Chauvin, M.-N. Collomb, D. Daveloose, A. Deronzier and J.-C. Leprêtre, *Eur. J. Inorg. Chem.*, 2005, 3320.
4. L. Sun, L. Hammarström, T. Norrby, H. Berglund, R. Davydov, M. Anderson, A. Börje, P. Korall, C. Philouze, M. Almgren, S. Styring and B. Akermark, *Chem. Commun.*, 1997, 607.
5. S. Romain, C. Baffert, S. Dumas, J. Chauvin, J.-C. Leprêtre, D. Daveloose, A. Deronzier and M.-N. Collomb, *Dalton Trans.*, 2006, 5691.
6. S. Romain, J.-C. Leprêtre, J. Chauvin, A. Deronzier and M.-N. Collomb, *Inorg. Chem.*, 2007, **46**, 2735.
7. A. Macatangay, G. Y. Zheng, D. P. Rillema, D. C. Jackman and J. W. Merkert, *Inorg. Chem.*, 1996, **35**, 6823.
8. R. Sahai, D. A. Baucom and D. P. Rillema, *Inorg. Chem.*, 1986, **25**, 3843.
9. A. K. Kirsch, A. Schaper, H. Huesmann, M. A. Rampi, D. Möbius and T. H. Jovin, *Langmuir*, 1998, **14**, 3895.
10. C. J. Kleverlaan, M. T. Indelli, C. A. Bignozzi, L. Pavanin, F. Scandola, G. M. Hasselman and G. J. Meyer, *J. Am. Chem. Soc.*, 2000, **122**, 2840.
11. M. Furue, K. Maruyama, Y. Kanematsu, T. Kushida and M. Kamachi, *Coord. Chem.*, 1994, **132**, 201.
12. B. Gholamkhass, H. Mametsuka, K. Koike, T. Tanabe, M. Furue and O. Ishitani, *Inorg. Chem.*, 2005, **44**, 2326.
13. X. Song, Y. Lei, S. Van Wallendal, M. W. Perkovic, D. C. Jackman, J. F. Endicott and D. P. Rillema, *J. Phys. Chem.*, 1993, **97**, 3225.
14. N. Komatsuzaki, Y. Himeda, T. Hirose, H. Sugihara and K. Kasuga, *Bull. Chem. Soc. Jpn.*, 1999, **72**, 725.
15. S. Van Wallendael, R. J. Shaver, D. P. Rillema, B. J. Yoblinski, M. Stathis and T. F. Guarr, *Inorg. Chem.*, 1990, **29**, 1761.

16. E. C. Sanudo, V. A. Grillo, M. J. Knapp, J. C. Bollinger, J. C. Huffman, D. N. Hendrickson and G. Christou, *Inorg. Chem.*, 2002, **41**, 2441, and references therein.
17. C. M. Elliott, D. L. Derr, D. V. Matyushov and M. D. Newton, *J. Am. Chem. Soc.*, 1998, **120**, 11714.
18. B. R. Serr, K. A. Andersen, C. M. Eliott and O. P. Anderson, *Inorg. Chem.*, 1988, **27**, 4499.
19. S. Ferrere and C. M. Eliott, *Inorg. Chem.*, 1995, **34**, 5818.
20. J. Lacour, J. J. Jodry and D. Monchaud, *Chem. Commun.*, 2001, 2302.
21. M. Tominaga, T. Kusukawa, S. Sakamoto, K. Yamaguchi and M. Fijita, *Chem. Lett.*, 2004, **33**, 794.
22. M.-T. Youinou, R. Ziessel and J.-M. Lehn, *Inorg. Chem.*, 1991, **30**, 2144.
23. G. Baum, E. C. Constable, D. Fenske, C. E. Housecroft and T. Kulke, *Chem. Commun.*, 1999, 195.
24. Y. Yao, M. W. Perkovic, D. P. Rillema and C. Woods, *Inorg. Chem.*, 1992, **31**, 3956.
25. C. O. Dietrich-Uchecker, J.-F. Nierengarten, J.-P. Sauvage, N. Armaroli, V. Balzani and L. De Cola, *J. Am. Chem. Soc.*, 1993, **115**, 11237–11244.
26. S. Bernhard, K. Takada, D. Jenkins and H. D. Abruña, *Inorg. Chem.*, 2002, **41**, 765.
27. S. Bernhard, J. I. Goldsmith, K. Takada and H. D. Abruña, *Inorg. Chem.*, 2003, **42**, 4389.
28. S. Ching and C. M. Elliott, *Langmuir*, 1999, **15**, 1491.
29. D. L. Feldheim, C. J. Baldy, P. Sebring, S. M. Hendrickson and C. M. Elliott, *J. Electrochem. Soc.*, 1995, **142**, 3366.
30. K. Gorgy, M.-N. Collomb, J.-C. Leprêtre, A. Deronzier, C. Duboc-Toia, S. Ménage and M. Fontecave, *Electrochem. Commun.*, 2001, **3**, 686.
31. R. Dobrawa and F. Würthner, *J. Polym. Sci., Part A: Polym. Chem.*, 2005, **43**, 4981.
32. P. R. Andres and U. S. Schubert, *Adv. Mater.*, 2004, **16**, 1043.
33. M.-N. C. Dunand-Sauthier, A. Deronzier, C. D. Toia, M. Fontecave, K. Gorgy, J.-C. Leprêtre and S. Ménage, *J. Electroanal. Chem.*, 1999, **469**, 53.
34. M.-N. Collomb, A. Deronzier, K. Gorgy and J.-C. Leprêtre, *New J. Chem.*, 2000, **24**, 455.
35. V. V. Pavlishchuk and A. W. Addison, *Inorg. Chim. Acta*, 2000, **298**, 97.
36. J. G. Eaves, H. S. Munro and D. Parker, *Inorg. Chem.*, 1987, **26**, 644.
37. P. Denisevich, H. D. Abruña, C. R. Leidner, T. J. Meyer and R. W. Murray, *Inorg. Chem.*, 1982, **21**, 2153.
38. A. Deronzier, J.-C. Moutet and D. Zsoldos, *J. Phys. Chem.*, 1994, **98**, 3086.
39. A. Deronzier, D. Eloy, P. Jardon, A. Martre and J.-C. Moutet, *J. Electroanal. Chem.*, 1998, **453**, 179.